JET–R(98)01

Numerical Code for LHCD Simulations with Self-consistent Treatment of Alpha Particles in Tokamak Geometry

A D Piliya, A N Saveliev.

JET Joint Undertaking, Abingdon, Oxfordshire, OX14 3EA,

February 1998

1. INTRODUCTION

In this report the development of a numerical model for studying interaction between LH waves and thermonuclear α-particles in tokamak geometry is described in view of the DT experiments on JET. Motivation for this work is the obvious fact that a considerable part of α-particles are born in a tokamak plasma as trapped particles. Their interaction with the LH waves can not be described accurately enough using the standard quasilinear (Fokker-Planck) approach. In fact, the RF effect on the α-particles is adequately described as the quasilinear diffusion in the space of variables which are constants of drift motion. In an axisymmetrical magnetic configuration, particle drift orbits are determined by three independent integrals of motion which can be, for example, the particle energy, the transverse adiabatic invariant and the canonical toroidal momentum. Adding to that the fast ion spatial diffusion makes the problem at least four-dimensional. This seems much too difficult for any comprehensive analysis. To keep the computer run time and required memory amount for numerical calculations within acceptable limits one is forced to sacrifice a part of the full description.

In the model adopted in this work, no spatial diffusion is assumed and the “thin banana” approximation is used. This reduces calculation of the fast ion distribution function to solving a two-dimensional Fokker-Planck equation for each radial grid point.

The computational basis of this work is an improved version of the fast ray tracing code (FRTC) described in Ref.[1]. The most important modifications of the code are the possibility to use arbitrary equilibrium configurations, including those with X-points and a module permitting self-consistent treatment of α-particles with the use of the 1D model of Ref.[2].

The report is organized as follows. Calculation of the magnetic toroidal coordinates is described in Sec.2. For the reader’s convenience, the ray tracing procedure is outlined in Sec.3, following Ref.[1]. Section 4 is devoted to the alpha particle treatment. It includes discussion of the model, formulation of the Fokker-Planck equation, analytical investigation of the limiting cases and outline of the used numerical approach. Finally, numerical calculations for JET conditions and conclusions are given in Sec. 5.

2. EQUILIBRIUM AND COORDINATES

In this code all calculations are performed in toroidal coordinates related to the tokamak magnetic field. The code itself, however, does not compute required equilibrium configurations. Instead, an equilibrium determined independently is used as external input. The equilibrium codes usually present their output data in a convenient laboratory coordinate system. To make these data available, the simulation code has a program finding the toroidal coordinates for a given equilibrium. In this Section, the method used for this purpose is described. The problem can be

formulated as follows. Introduce in the meridian tokamak cross-section general coordinates r, θ, with $r \geq 0$ and $0 \leq \theta \leq 2\pi$, related to the Cartesian coordinates x,z by

$$\begin{aligned} x &= x_0 + aX(r,\theta) \\ z &= z_0 + aZ(r,\theta) \end{aligned} \tag{2.1}$$

here the x axis is directed along the major radius, x_0, z_0 denote the magnetic axis position, the "minor radius" a is the last magnetic surface half-width and $X(r,\theta)$, $Z(r,\theta)$ are arbitrary functions. Fix these functions by the demand that curves described by Eq.(2.1) at r=const and θ varying from zero to 2π coincide, for all r, with the flux surfaces contours of the real magnetic configuration. Then the quantities r, θ given by Eq.(2.1), together with the toroidal angle φ, are the sought magnetic coordinates with the "radius" r denoting the magnetic flux surface and θ being the poloidal generalized angle at this surface. In fact, required coordinate transformation can be found only approximately with the use of the best-fit procedure.

Consider, first, equilibrium having up-down symmetry and no X-points. In this case, a satisfactory result is obtained for any conventional tokamak configuration with $X=X_0$, $Z=Z_0$, where

$$\begin{aligned} X_o &= r\cos\theta - \Delta(r) + \gamma(r)\sin^2\theta \\ Z_o &= r\lambda(r)\sin\theta \end{aligned} \tag{2.2}$$

Here the functions Δ, λ and γ characterize the Shafranov shift, ellipticity and triangularity of the flux surface r=const, respectively. These functions together with the function $r(\Psi)$ where Ψ is the poloidal flux, are found in the following way. First, for N, typically 100, flux surfaces $\Psi(x,z)=\Psi_i$ values of the parameters r_i, $\Delta_i=\Delta(r_i)$, $\lambda_i=\lambda(r_i)$, $\gamma_i=\gamma(r_i)$ are determined demanding extreme points of "theoretical" curves of Eqs.(2.1)-(2.2) to coincide with extreme points of the real flux surface contours. These calculations are performed explicitly; in particular, they give r=1 for the last magnetic surface. Then, each four sets of N found points are fitted, using the least-square method, to a polynomial of r with prescribed, if necessary behavior at $r \to 0$.

Consider now an equilibrium with a single X-point. Since the flux Ψ has a singularity in this point, we amend the functions X and Z by singular terms which describe correctly the field behavior in the immediate vicinity of the X-point within the separatrix:

$$\begin{aligned} X &= X_0 + \Phi_X \\ Z &= Z_0 + \Phi_Z \end{aligned} \tag{2.3}$$

Here

$$\begin{aligned} &\Phi_i = [A_i + B_i\sqrt{s}]\exp(-C_i s_1) + D_i^{(N)}, \qquad (i = x, z) \\ &s = 1 - \cos(\theta - \theta_*) + \alpha(1-r), \qquad s_1 = 2 - \cos(\theta - \theta_*) - r \end{aligned} \tag{2.4}$$

with A_i, B_i, α and C_i being r-independent constants, and $D_i^{(N)}$ is a N-th order trigonometric polynomial with r-dependent coefficients. The θ_* parameter is the angular coordinate of the X-point on the separatrix r=1. This parameter can be chosen arbitrary. Assuming, for certainty, that the X-point is located in the lower half-plane z<0, we put, for convenience, $\theta_*=3\pi/2$. Fitted parameters and functions in the coordinate transformation Eq.(2.3) are found iteratively. First, the functions $r(\Psi)$, Δ, λ and γ are determined ignoring the functions Φ and applying above procedure to the upper part of the magnetic configuration at z>0. In further fitting process these functions are hold unchanged. In the next step, parameters A_i, B_i which control location of the X-point and direction of the separatrix branches are fixed. Since only a small angular interval around the $\theta_*=3\pi/2$ is involved at this stage, results are insensitive to the parameters C_i and the calculations are performed with C_i=0. Then, ignoring the D_i terms, values of the parameters C_i, minimizing the mean-squared difference between real and "theoretical" separatrix are found. Having the separatrix properly described, the parameter α is adjusted to guarantee exact spatial location of the point $\theta=\theta_*$ on a flux surface close to the separatrix, typically, with r=0.8. This takes account of a correct description of the field in the boundary layer. Finally, optimum values of coefficients in the functions $D_i^{(N)}$ are found at 10 flux surfaces with the use of the least-square method and fitted to second-order polynomials of r. Because of the relative simplicity of the coordinate transformation Eq.(2.3) and step by step fitting routine finding the magnetic coordinates is rather fast.

Results obtained with this procedure for a typical JET equilibrium are illustrated in Fig.1 for flux surfaces and in Fig.2 for the poloidal magnetic field which is much more sensitive to the accuracy of used approximations.

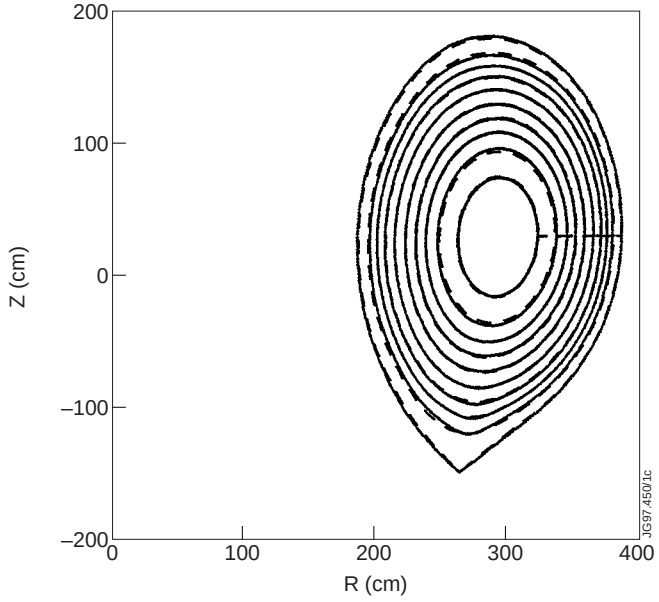

Fig.1. Poloidal flux surfaces for a typical JET equilibrium. Dashed lines are from the numerical solution of the Grad-Shafranov equation, solid lines from Eq.(2.3)

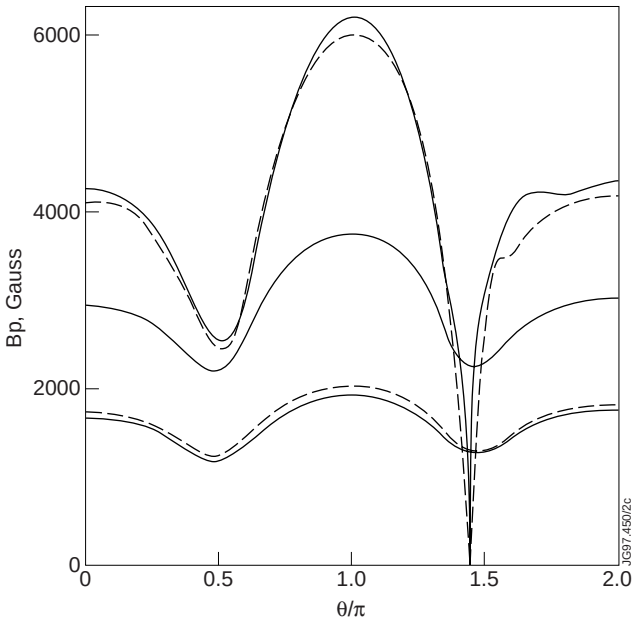

Fig.2. Poloidal magnetic field for the case of Fig.1. on three flux surfaces.

3. RAY TRACING PROCEDURE

In order to proceed with the ray calculations, one has to specify spatial co-ordinates q_i (i=1, 2, 3) and express the left hand side of the dispersion relation H=0 in terms of these co-ordinates and the canonical conjugate momenta p_i. Then ray trajectories in the phase space (p,q) obey the canonical equations

$$\frac{dq}{dt} = \frac{\partial H}{\partial p} \quad \frac{dp}{dt} = -\frac{\partial H}{\partial q} \tag{3.1}$$

The code uses coordinates described in Sec.2 with $q_1=r$, $q_2=\theta$, $q_3=\varphi$. The canonical momenta are denoted as k_r, m, n, respectively. Assuming an axisymmetric tokamak plasma geometry φ becomes a cyclic variable and n a constant of motion. Then Eqs.(3.1) are reduced to a system of four equations for r, k_r, θ and m. This system, together with the power evolution equation, is solved numerically in all known ray tracing codes. In the present code, however, we utilize a different representation of ray equations taking the radial coordinate as the independent variable. To perform a transformation to this variable one has to find $k_r=K(r,\theta,m)$ from the dispersion relation and use K as a Hamiltonian function in canonical equations for $\theta(r)$ and $m(r)$:

$$\frac{d\theta}{dr} = -\frac{\partial K}{\partial m} \qquad \frac{dm}{dr} = \frac{\partial K}{\partial \theta} \tag{3.2}$$

Unlike the initial Hamiltonian function H, the new Hamiltonian K is not preserved along the ray. In the present version of the code we calculate the rays using the cold plasma approximation for the background plasma and considering the α-particles as a small minority, *i.e.* neglecting their contribution in the real part of the dispersion relation. Then the latter takes the form

$$\varepsilon_\perp n_\perp^4 - \left[(\varepsilon_\perp + \varepsilon_{ll})(\varepsilon_\perp - n_{ll}^2) - g^2\right] n_\perp^2 + \varepsilon_{ll}\left[(\varepsilon_\perp - n_{ll}^2)^2 - g^2\right] = 0 \tag{3.3}$$

where $\varepsilon_\perp=\varepsilon_{xx}$, $\varepsilon_{ll}=\varepsilon_{zz}$ and $g=-i\varepsilon_{xy}$ are the non-vanishing elements of the cold plasma dielectric tensor in the coordinate system with the z axis along the magnetic field. Then the new Hamiltoninan function K is given by an explicit expression. The thermal corrections should be added to the term $\varepsilon_\perp n_\perp^4$ in the dispersion relation close to the lower hybrid resonance $\varepsilon_\perp=0$ that makes the determination of the Hamiltonian K more difficult. We do not consider this case here, assuming the wave frequency ω to be sufficiently high. The cold plasma dispersion relation has at most four real roots K_j, (j=1, 2, 3, 4) which represent the slow and the fast wave modes propagating in opposite directions. The root must be specified at the starting point of a ray together with the initial values of m and θ. The selected branch of the Hamiltoninan function K is to be used in

Eqs.(3.2) until a “root intersection point” is reached. The intersection occurs at points where two roots of the dispersion relation merge. It corresponds to a cut-off when merging roots belong to the same type of wave modes or to a slow-fast (fast-slow) linear conversion in the opposite case. Since the radial ray direction always changes at the root intersection points, these points can be generally called “the turning points”. The ray is to be followed using the new branch of K after each intersection. Therefore, the root number j is an additional variable changing its value at isolated points along a ray. Representation of the ray equation in the form of Eqs(3.2) has proved to be very helpful. First of all, the ray calculations can now be performed directly on the radial grid prescribed for presentation of the RF driven current profile. More importantly, reducing the number of ray equations from four to only two permits one to utilize with high efficiency the Richardson-Bulirsch-Stoer (RBS) method Ref.[3] for solving them. In this method, a sequence of separate attempts to cross the interval $h=r_{k+1}-r_k$ (where k is the flux surface number) is made with an increasing number of substeps. The final answer is found by effective extrapolation of the intermediate results obtained in these attempts to zero substep size. This procedure, applied to Eqs(3.2), speeds up the calculations considerably. However, it has difficulties in dealing with the root intersection points. The program recognizes the approach to an intersection point from the current ray data and abandons the RBS procedure. Tracing is performed in a narrow vicinity of the point by using the regular Runge-Kutta solution of four equations. Then the program returns back to the fast computational mode (the RBS procedure). The relative lengths of the trajectory portions traced with the Runge-Kutta method are short. Nevertheless, they consume about half of the CPU time in a typical computer run. Although the described numerical procedure may seem rather formidable, it actually works very effectively and provides a significant part of the code speed enhancement.

The RF power P_i assigned to the i-th ray is calculated in parallel with ray tracing from the relation

$$P_i(r_{k+1}) = P_i(r_k)\exp\left(\int_{r_k}^{r_{k+1}} 2\kappa\, dr\right) \tag{3.4}$$

where κ is the spatial damping rate. It consists of three parts, $\kappa=\kappa_{Le}+\kappa_{\alpha}+\kappa_C$, resulting from electron Landau damping, hot ion damping and Coulomb collisions, respectively. The κ_{Le} term here has the form

$$\kappa_{Le} = \Gamma \frac{\partial f}{\partial v} \tag{3.5}$$

with f being the one dimensional ("parallel") electron distribution function normalized to unity and Γ is independent of f:

$$\Gamma = -\pi c \frac{\omega_{pe}^2}{\omega} n_\perp^2 \left(\frac{\partial n_\perp^2}{\partial n_r} \left[\varepsilon_{ll} n_{ll}^2 + g^2 \frac{\left(n_\perp^2 - \varepsilon_{ll}\right)^2}{\left(n^2 - \varepsilon_\perp\right)^2} \right] \right)^{-1} \tag{3.6}$$

Each individual ray is followed until its assigned power falls below a prescribed value.

The flux surface averaged electron quasilinear diffusion coefficient D_e is calculated on each flux surface r_k on a flexible v grid. To set limits to the grid we fix lower and upper extreme points of the v axis reached by any of the rays in each iteration. If either of these points happens to lie outside the existing grid, it is taken as a new extreme grid value; in the opposite case the v range remains unchanged.The v grid is divided into two intervals having different spacings, that at lower v being finer. The quasilinear diffusion coefficient D_e is determined from the relation

$$Q_L = n_e m_e D_e v \frac{\partial f}{\partial v} \tag{3.7}$$

where $Q_L(r,v)$ is the flux surface averaged RF power absorbed by plasma electrons via Landau mechanism. The RF power going to electrons is found from

$$Q_L = \frac{\mathbf{1}}{\Delta V_k \Delta v_n} \sum_{i,j} \Delta P_{ijkn} \tag{3.8}$$

where ΔV_k is the volume between the flux surfaces represented by radial co-ordinates r_{k+1} and r_k, $\Delta v_n = v_{n+1} - v_n$ is the interval between the $(n+1)$-th and n-th points of the v axis, ΔP_{ijkn} is the power lost by the ray in its j-th transit through the phase space element $\Delta V_k \Delta v_n$ due to the Landau damping and summation over rays and transits. The RF power P_i varies smoothly over most of the ray, therefore power calculations using Eq.(3.4) with the fixed step size present no problem in nearly the entire phase space. The only exception may be the small-v region where γ_{Le} increases sharply. One can expect that as P_i varies very rapidly here, the adopted r-grid spacing is too coarse to guarantee the necessary accuracy in power deposition calculations. However, this is not the case. In fact, behaviour of the distribution function f close to the lower boundary of the quasilinear plateau can be investigated analytically, independently of the ray tracing. The analysis shows that the diffusion coefficient D_e is practically a linear function of v in the region of interest. As a result the described procedure provides a reliable self-consistent solution for the electron distribution function and the diffusion coefficient at all v and r.

A self-consistent relation between the diffusion coefficient and the electron distribution function is found in an iteration process that involves the Fokker-Planck and power evolution equations. The ray data necessary for these calculations include four quantities: flux surface number, velocity v, collisional damping rate γ_C and coefficient Γ. These quantities are calculated in sequence for all rays and stored in four arrays in the form of a linear structure. More detailed information concerning the last point of each ray is also recorded. If the length of any particular ray increases in the iteration process due to a change of the electron distribution function, a new fragment is calculated using this as the initial condition and stored in the same array. This operation can be repeated for each ray as many times as necessary.

For each step of the iteration process the CPU time is mostly determined by the total length of the newly calculated ray pieces. Typically, the ray length is a maximum at the Maxwellian electron distribution and decreases as the quasilinear plateau is formed. Therefore, the first iteration consumes most of the total run time when the initial distribution function is a Maxwellian. To avoid calculation of excessive ray fragments at earlier stages of iteration, we may artificially limit the ray length, increasing it gradually until rays are allowed to live their natural lifetime. In this scenario, the total CPU time is reduced and distributed more uniformly over the iteration steps.

The iteration convergence deteriorates dramatically in certain tokamak regimes due to the presence of “overlong rays”. These regimes are characterized by a large number of small islands in the phase space of the ray equations. A finite fraction of ray trajectories is launched inside the islands and remains confined there with nearly constant $N_{||}$. These rays, practically unaffected by Landau damping, have extremely long lengths. In spite of their relatively small number and negligible contribution to the current density, the overlong trajectories consume a considerable part of the CPU time and are even capable of making the ray tracing impossible. To cope with this problem, the code uses a special procedure for selecting the overlong rays. If the return of the trajectory to a small vicinity of its starting point occurs periodically for a given number of times, the ray is identified as overlong and terminated. This procedure may be helpful in certain cases.

A simple 1-D model of the electron Fokker-Planck equation is used in the code to avoid time consuming numerical solution of a partial differential equation in the iterative cycle.

4. MODEL FOR ALPHA PARTICLES

Fokker-Planck equation

The quasilinear diffusion of ions interacting with the LH waves is discussed in some detail in the literature Refs.[2, 4] for the case of cylindrical geometry with uniform magnetic field. Including toroidal effects requires certain modification in the approach which we briefly outline in this section.

An important feature of interaction between energetic ions and RF fields in tokamaks is the fact that the particle's transit time is very small in both collisional and quasilinear time scales. For example, in typical JET regimes the difference is more than 6 order of magnitude for thermonuclear α-particles. In these conditions, the quasilinear effect of the RF field is effectively averaged over particle orbits. Then it is natural to describe the α-particle population in terms of variables that are constants of motion in the absence of the RF field. Transition to these variables means that we consider quasi-particles represented by a proper fragment of the orbit (by the "banana" in the case of the trapped ions) rather than by the particles themselves, in the same way as the cyclotron circles are treated in the drift theory. The unperturbed particle motion in a tokamak is adequately described by the drift approximation. Then, in an axisymmetrical configuration, an orbit is determined by three integrals of drift motion. To reduce the number of variables and thus make the problem treatable for the code intended for routine computation, we assume that the unperturbed motion is along the field lines. In this approximation which ignores passing particle excursions from the flux surfaces and finite "banana" width for trapped particles, an orbit is fully determined by two constants of motion. They may be chosen in various ways, for example, $\varepsilon=v^2$ and the transverse adiabatic invariant $\mu=v_\perp^2/H$ can be used. The most preferable variables are, however, $v_{\perp 0}$ and $v_{\|0}$ which are values of $v_\perp$ and $v_\|$ at the extreme low field point of the orbit. For further simplification, we also assume the absence of the fast ion spatial diffusion. Then it is convenient to consider α-particles confined in a shell between flux surfaces r, $r+\Delta r$ and introduce the function $F(v_{\perp 0},v_{\|0},r)$ describing their distribution over integrals of motion. The argument r of the function is actually a parameter denoting the shell.

Having the function F known, the "usual" α-particle distribution function $f_\alpha(v_\perp,v_\|,r,\theta)$ which is the particle phase space density can be easily found (see Eq.(4.20)). This function is required, in particular, for the calculation of the wave damping. The steady-state distribution function $F_\alpha(v_{\|0},v_{\perp 0})$ satisfies the Fokker-Planck equation

$$\frac{\partial \mathbf{S}}{\partial \mathbf{v}_0} = Q(v_{\|0}, v_{\perp 0}) \tag{4.1}$$

where the right-hand side describes the birth of α-particles within the shell volume and the left-hand side is the divergence in the $(v_{\perp 0}, v_{\|0})$ space of the flux $\mathbf{S}=\mathbf{S}^C+\mathbf{S}^{QL}$ resulting from collisions and RF diffusion respectively. The equation implies a sink at $v\to 0$. We begin with the RF induced flux $\mathbf{S}^{QL}$. Generally, two-dimensional diffusion is determined by a diffusion tensor D_{ik}, (i, k=1, 2), where the subscripts 1 and 2 refer to the perpendicular and the parallel directions, respectively. We find the diffusion tensor heuristically, using the random walk approximation. To this end, we calculate in the linear approximation variations $\Delta v_{\perp 0}(T)$ and $\Delta v_{\|0}(T)$ of $v_{\perp 0}$ and $v_{\|0}$ resulting from the particle interaction with the RF field during the time interval T and define

$$D_{11}=\frac{\langle v_{\perp 0}^2\rangle}{2T}, D_{12}=\frac{\langle \Delta v_{\perp 0}\Delta v_{ll0}\rangle^2}{2T}, D_{22}=\frac{\langle \Delta v_{ll0}^2\rangle}{2T} \tag{4.2}$$

where, in the spirit of the quasilinear theory, variations $\Delta v_{\perp 0}(T)$ and $\Delta v_{l0}(T)$ are supposed to be random quantities and the symbol $\langle\ \rangle$ denotes the ensemble averaging. To find the velocity variations consider a particle with given values of $\mu=v_\perp{}^2/H$ and $\varepsilon=v^2$ and suppose that it experiences an instant random "kick" in a moment of time $t=t_i$ resulting in a variation $\Delta v_\perp$ of $v_\perp$. Then μ and ε also change with

$$\delta\mu = 2\sqrt{\mu}\frac{\delta v_\perp}{\sqrt{H_i}} \tag{4.3}$$

and

$$\delta\varepsilon = H\delta\mu = 2\sqrt{\mu H_i}\delta v_\perp \tag{4.4}$$

where $H_i=H(r,\theta(t_i))$. Assuming that the "kicks" are generated continuously, we can calculate, in linear approximation, total changes in ε and μ over the time interval T, which includes many bounce periods:

$$\Delta\mu = 2\sqrt{\mu}\oint_T \frac{\delta v_\perp(t)}{\sqrt{H(t)}}dt \tag{4.5}$$

and

$$\Delta\varepsilon = 2\sqrt{\mu}\oint_T \delta v_\perp(t)\sqrt{H(t)}dt \tag{4.6}$$

where $H(t)=H(r,\theta(t))$ and the integration is performed along the unperturbed orbit. Now, using definition of μ and ε, the required variation of $v_{\perp 0}$ and v_{ll0} can be found:

$$\Delta v_{\perp 0} = \oint_T \frac{\delta v_\perp(t)}{\sqrt{h(t)}}dt \tag{4.7}$$

$$\Delta v_{ll0} = \frac{v_{\perp 0}}{v_{ll0}}\oint_T\left(\sqrt{h}-\frac{1}{\sqrt{h}}\right)\delta v_\perp(t)dt \tag{4.8}$$

here $h=H/H_{min}$ with H_{min} being the minimum value of the magnetic field on the flux surface. Considering $\Delta v_{\perp}(t)$ as a random function we see that the random quantities $\Delta v_{\perp 0}$ and Δv_{ll0} are not related functionally, although they are statistically correlated. This means that the random walk is essentially two-dimensional and can not be reduced to one-dimensional diffusion along lines in the ($v_{\perp 0}$, v_{ll0}) plane.

Supposing the correlation time of the velocity variations to be short compared to the integration time T, we can put

$$\langle \delta v_{\perp}(t)\delta v_{\perp}(t')\rangle = D_0\delta(t-t') \tag{4.9}$$

to obtain

$$D_{11} = \frac{1}{T}\oint \frac{D_0}{h}dt \tag{4.10}$$

$$D_{22} = \left(\frac{v_{\perp 0}}{v_{ll}}\right)^2 \frac{1}{T}\oint (h-1)^2 \frac{D_0}{h}dt \tag{4.11}$$

$$D_{12} = \frac{1}{T}\left(\frac{v_{\perp 0}}{v_{ll}}\right)\oint (h-1)\frac{D_0}{h}dt \tag{4.12}$$

The quantity D_0 here is, obviously, the local diffusion coefficient. This can be easily confirmed by the direct calculation. We should find $\Delta v_{\perp}$ from the linearized equation of motion in the presence of the RF field. For LH waves having $k_{\perp}>>k_{ll}$, $E_{\perp}>>E_{ll}$ and $k_{\perp}v_{\perp}/\omega_{c\alpha}>>1$, where $\omega_{c\alpha}$ is the α-particle cyclotron frequency, the "kick" from the field component with a given $k_{\perp}$ is generated at the points of particle orbit where the Landau resonance condition

$$k_{\perp} v_{\perp 0}(t) = \omega \tag{4.13}$$

is locally satisfied. The contribution of an individual resonance is calculated in a straight-forward way. Then, making standard quasilinear theory assumptions concerning the RF field we obtain

$$D_0(v_{\perp}) = \frac{Z_{\alpha}^2 e^2}{m_{\alpha}^2 \omega}\int dn_{ll} \frac{\left|E_{\perp}(n_{ll})\right|^2}{\left(1-\left(c^2/n_{\perp}^2 v_{\perp}^2\right)\right)^{1/2}}\left(\frac{c}{n_{\perp}v_{\perp}}\right)^3 \tag{4.14}$$

Here $\left|E_{\perp}\right|^2$ is a local value (depending on spatial coordinates r,θ,φ) of the LH perpendicular spectral density, $n_{ll}=k_{ll}c/\omega$, $n_{\perp}=k_{\perp}c/\omega$ with $n_{\perp}$ being a function of n_{ll} determined by the LH

dispersion relation, $v_\perp=\sqrt{h}v_{\perp 0}$, Z_α and m_α are the charge number and the mass of the fast ions and integration performed over the n_{ll} region where $\left(c^2 / n_\perp^2 v_\perp^2\right)<1$. The function $D_0(v_\perp)$ in Eq.(4.14) is the familiar RF diffusion coefficient. To proceed with the calculation of the diffusion tensor we may replace the time integration in Eqs (4.10)-(4.12) by the integration along the field line which, in turn, can be transformed, under condition $T>>T_B$ where T_B is the bounce period, into integration over the flux surface:

$$\frac{1}{T}\int \ldots dt \to \int \ldots W(\theta) dS \tag{4.15}$$

where W(θ) is a weight function normalized to unity. This expression implies that the orbit goes many times round the torus during the integration time. Passing particles make these rotations following the field lines. For trapped particles net toroidal displacement is due to precession of "banana" orbits and the transit time is increased by a factor r/ρ_α, where ρ_α is the α-particle gyroradius. Nevertheless, it remains sufficiently small for Eq.(4.15) to be still valid. To find the weight function we note that

$$2\pi R(\theta) W \sqrt{g_{22}} d\theta = \frac{dt}{T_B} \tag{4.16}$$

where dt in the right-hand side is the time which a particle spends within the poloidal angle interval $d\theta$ during a single bounce period T_B and g_{22} is the metric tensor element. Then with the use of the relation

$$\sqrt{g_{22}} \frac{d\theta}{dt} \equiv v_p = v_{ll} \frac{H_p}{H} \tag{4.17}$$

we obtain:

$$W(\theta) = \frac{1}{T_B} \frac{H}{H_p \; 2\pi R v_{ll}} \tag{4.18}$$

with

$$v_{ll} = \sqrt{v_{ll0}^2 - v_{\perp 0}^2 (h-1)}$$

The bounce period can be now written in the form

$$T_B = \oint \frac{H}{H_p} \frac{\sqrt{g_{22}}}{v_{ll}} d\theta \tag{4.19}$$

For the elements of the diffusion tensor we obtain

$$D_{ik} = \oint_{S(r)} \frac{\Lambda_{ik} D_0 W}{h} ds \tag{4.20}$$

where $\Lambda_{11}=1$, $\Lambda_{12}=h\text{-}1$, $\Lambda_{22}=(h\text{-}1)^2$ and the integration is performed over the flux surface $r=const$. Having the diffusion tensor found is still insufficient for formulation of the Fokker-Plank equation. The problem here lies in the fact that the averaging according to Eq.(4.20) and the v_0 differentiations are non-commutative operations. Therefore, the result depends on the position of the diffusion tensor elements (or, generally, of any v-dependent factors) relative to differential operators in the flux expression. The explicit form of the quasilinear operator in Eq.(4.1). can be found in the following way. Consider, along with the function $F(v_{\perp 0}, v_{ll0})$ also the phase density $f_\alpha(v_{\perp 0}, v_{ll0}, \theta)$. It can be easily shown that these functions are related by

$$f_\alpha = \frac{H_0}{\psi' \Delta r T_B v_{ll0}} F \tag{4.21}$$

where $\psi' \Delta r$ is the poloidal flux confined within the shell. The expression $\Delta V = dSdl$, where $dl = \psi' \Delta r / 2\pi R H_p$ is the local thickness of the shell, has been used for the shell volume in the Eq.(4.21) derivation. According to the above analysis, effect of the RF field on the α-particles can be described as the "local" quasilinear diffusion given by the operator

$$\frac{1}{v_\perp} \frac{\partial}{\partial v_\perp} \left(v_\perp D_0 \frac{\partial f_\alpha}{\partial v_{\perp 0}} \right) \tag{4.22}$$

Let us calculate now the variation rate δN_α of the particle number within the shell volume in the velocity interval dv_0 due to the quasilinear difusion. Expressing this quantity in terms of the functions F and f_α respectively, we can write, by difinition,

$$\frac{\partial \mathbf{S}^{QL}(F)}{\partial \mathbf{v}_0} = \int dV \left[\frac{1}{v_\perp} \frac{\partial}{\partial v_\perp} \left(v_\perp D_0 \frac{\partial f_\alpha}{\partial v_{\perp 0}} \right) \right] \frac{dv}{dv_0} \tag{4.23}$$

where dv/dv_0 is the Jacobian of the coordinate transformation and integration is performed over the shell volume. Direct, although rather tedious calculation of the integral with the use of Eqs.(4.18)-(4.20) represents it in the form of the left-hand side of Eq.(4.23) with

$$\mathbf{S}^{QL} = (\nu_{ll0} T_B) \hat{D} \frac{\partial}{\partial \mathbf{v}_0} \left(\frac{F}{\nu_{ll0} T_B} \right) \tag{4.24}$$

where $\hat{D}$ is the diffusion tensor with the elements D_{ik}. This expression determines the RF induced flux of the α-particles.

Consider now the collisional flux $\boldsymbol{S}^C$. The effect of the Colomb collisions on energetic ions can be described as a superposition of the velocity space diffusion due to the pitch-angle scattering and the slowing down resulting from the dynamical friction between the ions and background plasma electrons. The relative role of these two processes depends on the relation between the fast ion velocity v and the critical velocity v_c given by

$$v_c = \left(3\sqrt{\frac{\pi}{2}} \tilde{Z} \frac{T_e^{3/2}}{m_p \sqrt{m_e}} \right)^{1/3} \approx 0.09 v_{T_e} \tag{4.25}$$

At $v \cong v_c$ both pitch-angle scattering and slowing down must be included, at $v^3 >> v_c^3$ the slowing down dominates and the pitch-angle scattering can be ignored. Now we note that only α-particles having sufficiently high velocity interact with the LH waves. According to Eq (4.13), the necessary condition for the quasilinear diffusion of a particle with a given $v_\perp$ is the presence of the waves having $\omega/k_\perp < v_\perp$ in the spectrum. However, the minimum perpendicular phase velocity $\omega/k_\perp$ is limited, since $k_\perp$ is related to k_{ll} via the dispersion relation and k_{ll} is limited due to the electron Landau damping:

$$\left(\frac{\omega}{k_{ll}} \right)^2 > 5 v_{T_e} \tag{4.26}$$

where $v_{T_e}^2 = 2T_e / m_c$. Using for estimation the electrostatic approximation for $k_\perp$, we obtain for the minimum value v_* of the phase velocity $\omega/k_\perp$ the expression

$$v_* = \sqrt{5} v_{T_e} \omega / \omega_{pe} \tag{4.27}$$

Only the α-particles with $v_\perp > v_*$ experience the quasilinear diffusion. Comparing v_* with the critical velocity v_c we conclude that under the condition $\omega/\omega_{pD} > 2.5$ which is readily satisfied

in LHCD experiments, the pitch-angle scattering is negligible for these particles. Here ω_{pD} is the deuterium ion frequency which is close to the lower hybrid frequency in low-density regimes typical for LHCD experiments. Since particles born with $v_\perp<v_*$ drift irreversibly downward in the velocity space, the interaction between thermonuclear α-particles and the LH waves only occurs at $v_*<v_\alpha$. This inequality can be written as $\omega/\omega_{pD} < 20/\sqrt{T_e}$ where the electron temperature is in *keV*.

Coming back to the calculation of the flux $\mathbf{S}^C$, we must find changes in $v_{\perp 0}$ and v_{ll0} produced by the collisions during the time interval *T*. The slowing down rate due to dynamical friction is given by $d\mathbf{v}/dt = -\nu\,\mathbf{v}$ where ν is the collision frequency

$$\nu = \frac{4\sqrt{2\pi}}{3}\frac{e^4 n_e}{T_e^{3/2}}\frac{Z_\alpha^2\sqrt{m_e}}{m_\alpha}\ln\Lambda \tag{4.28}$$

with lnΛ being the Colomb logarithm. Supposing that $\nu T<<1$ we find $\Delta\varepsilon^c=-\nu T\varepsilon$, $\Delta\mu^c=-\nu T\mu$, where the superscript "c" stands for "collisional". Then similar expressions also follow for $v^c_{\perp 0}$ and v^c_{ll0}: $\Delta v^c_{\perp 0}=-\nu T v_{\perp 0}$, $\Delta v^c_{ll0}=-\nu T v_{ll0}$. Now neglecting the pitch-angle scattering we can write the collisional flux $\mathbf{S}^C$ in the form:

$$\mathbf{S}^C = -\nu\,\mathbf{v}_0 F \tag{4.29}$$

To formulate finally the Fokker-Planck equation for the distribution function $F(v_{\perp 0},v_{ll0})$ we have to obtain the expression for the α-particle source $Q(v_{\perp 0},v_{ll0})$. The source represents the α-particle birth-rate in the volume between flux surfaces *r*, $r+\Delta r$ per unite volume in the velocity space$(v_{\perp 0}, v_{ll0})$. A straight-forward calculation gives

$$Q = \frac{\psi'\Delta r T_B v_{ll0}}{H_{\min}}\frac{\dot{N}}{4\pi v_\alpha^2}\delta\left(v - v_\alpha\right) \tag{4.30}$$

where $\dot{N}$ is an α-particle birth-rate per unite volume. Now, collecting Eqs.(4.1),(4.2) and (4.29) we can finally write the Fokker-Planck equation

$$\frac{1}{v_{\perp 0}}\frac{\partial}{\partial v_{\perp 0}}\left\{v_{\perp 0}\left[D_{11}\frac{\partial F}{\partial v_{\perp 0}} + D_{12}\frac{\partial F}{\partial v_{ll0}} + w_{\perp 0}F\right]\right\} + \frac{\partial}{\partial v_{ll0}}\left\{D_{22}\frac{\partial F}{\partial v_{llo}} + D_{21}\frac{\partial F}{\partial v_{\perp 0}} + w_{ll0}F\right\} = Q\left(v_{\perp o}, v_{ll0}\right) \tag{4.31}$$

Unlike the cylindrical geometry case, Eq (4.31) can not be integrated over v_{ll} to obtain an ordinary differential equation of an 1-D distribution function.

Computation of the alpha-particle quasilinear diffusion coefficient

The a-particle diffusion tensor is computed using a procedure which is a direct generalization of one employed in the electron calculations and described in Sec.3. According to Eqs.(4.15) and (4.20), the perpendicular spectral density $|E_\perp(n_\parallel)|^2$ integrated with a proper weight over n_{ll}, ϕ and θ, is required to find the diffusion tensor. Two of these integrations are performed in parallel with ray tracing in the following way. Each shell between flux surfaces is additionally splitted into toroidal cells with the poloidal angular size $\Delta\theta$. The electron diffusion coefficient D_e is found for each cell separately using Eqs.(3.7) and (3.8) with the shell volume ΔV_k replaced by the cell volume ΔV_{kl} where the subscripts k and l refers to the shell number and the cell number, respectively. This quantity, being local with respect to the radius and the poloidal angle, is averaged over the toroidal angle φ. Then the φ-averaged parallel spectral density $<|E_{ll}(n_{ll},r_k,\theta_l\})|^2>_\varphi$ is obtained from the relation

$$D_e = \pi \frac{e^2 n_{ll}}{m_e^2 \omega} \left\langle \left| E_{ll}\left(n_{ll}, r\right) \right|^2 \right\rangle \tag{4.32}$$

Further, the φ averaged perpendicular spectral density is determined with the use of the expression

$$\left| E_\perp \left(n_{ll}\right) \right|^2 = \frac{\left(n_\perp^2 - \eta\right)\left[\left(n^2 - \varepsilon\right)^2 + g^2\right]}{n_\perp^2 n_{ll}^2 \left(n^2 - \varepsilon\right)^2} \left| E_{ll}\left(n_{ll}, r\right) \right|^2 \tag{4.33}$$

Finally, $<|E_\perp(n_{ll},r_k,\theta_l)|^2>_\varphi$ is multiplied by the factor

$$\frac{Z_\alpha^2}{\pi} \frac{m_e^2}{m_\alpha^2} \left(\frac{1}{\left(1 - \left(c^2 / n_\perp^2 v_\perp^2\right)\right)^{1/2}} \right) \left(\frac{c}{n_\perp v_\perp} \right)^3$$

taken in discrete points $v_{\perp,\rho}$ and integrated over n_{ll} by the n summing with the weight factor $(n_{ll}\Delta v_n/v_n)$. The values $D_0(v_{\perp,\rho},r_k,\theta_l)$ found in this way are stored in a 3D array. Remaining θ integration of Eq.(4.20) is performed numerically, as well as calculation of the bounce periods. Obtained elements of the diffusion tensor are stored in three 3D arrays to be used in the Fokker-Planck calculations.

The wave damping due to α-particles has to be included into the power deposition calculations in a self-consistent analysis. For the LH waves we have $E_\perp >> E_{ll}$. Further, in the co-ordinate system with $k_x=k_\perp$, $k_y=0$

$$E_x = \frac{n^2 - \varepsilon}{ig} \tag{4.34}$$

In nearly the whole plasma volume, n^2>>g and we can associate $E_\perp$ with E_x. Then the wave damping due to the α-particles is determined by the quantity ε''_α which is the α-particle contribution to the imaginary part of the ε_{xx}. For typical LH wave values of n_{ll} energetic ions are effectively unmagnitized. Using the well known expression for the dielectric tensor in a hot unmagnitized plasma we readily obtain

$$\varepsilon''_\alpha = -\frac{8\pi^2 Z_\alpha^2 e^2}{m_\alpha \omega^2} \int_{\omega/k_\perp}^{\infty} dv_\perp v_\perp^2 \left(\frac{\omega}{k_\perp v_\perp}\right)^3 \left(1 - \frac{\omega^2}{k_\perp^2 v_\perp^2}\right)^{-1/2} \frac{d\overset{)}{f}_\alpha}{dv_\perp} \tag{4.35}$$

where

$$\overset{)}{f}_\alpha(v_\perp, \theta) = \int_{-\infty}^{\infty} f_\alpha(v_\perp, v_{ll}, \theta) dv_{ll} \tag{4.36}$$

Using Eq.(4.29), it can be written

$$\overset{)}{f}_\alpha(v_\perp, \theta) = \frac{2H_0}{\Psi' \Delta r} \int_{v_{\perp 0}\sqrt{1-h}}^{\infty} \frac{F(v_{\perp 0}, v_{ll0})}{T_B \sqrt{v_{llo}^2 - v_{\perp 0}^2 (1-h)}} dv_{ll0} \tag{4.37}$$

with $v_{\perp 0} = v_\perp / \sqrt{h}$. Now, recalling that the rays are calculated in FRTC using the cold plasma approximation, an expression for α-particle contribution κ_α to the spatial damping rate can be readily obtained

$$\kappa_\alpha = \frac{\omega}{c} \varepsilon''_\alpha \left(n_\perp^2 - \eta\right)^2 \left(\frac{\partial n_\perp^2}{\partial n_r} \left[\eta n_{ll}^2 + g^2 \frac{\left(n_\perp^2 - \eta\right)^2}{\left(n^2 - \varepsilon\right)^2} \right] \right)^{-1} \tag{4.38}$$

The damping rate κ_α can also be presented in the form

$$\kappa_\alpha = -\frac{\Gamma}{\pi c^2} \frac{\omega^2}{\omega_{pe}^2} \frac{\left(n_\perp^2 - \eta\right)^2}{n_\perp^2} \varepsilon''_\alpha \tag{4.39}$$

where Γ is given by Eq.(3.6).

Analytical consideration

To make clear general features of the Fokker-Planck equation, we consider the simplest case of a circular large aspect ratio tokamak with $h=1+2\varepsilon \sin^2(\theta/2)$, where $\varepsilon=r/R<<1$ is the inverse aspect ratio. Also, we assume for simplicity that D_0 is independent of θ, $D_0=D_0(v_\perp)$. Then to the lowest order in ε we have from Eq.(4.20)

$$D_{ik} = D_0(v_\perp) g_{ik}(\kappa) \tag{4.40}$$

where $\kappa=v^2_{\|0}/2\varepsilon v^2_{\perp 0}$, $g_{11}=1$, g_{12}, g_{22} and T_B are expressed in terms of elliptic integrals. Particles with $\kappa>1$ are passing and those with $\kappa<1$ are trapped. We do not write down the explicit expressions for g_{12}, g_{22} and T_B. Instead, we consider two limiting cases. For $\kappa \to \infty$, that corresponds to the cylindrical limit, $g_{12}\sim\kappa^{-1}$ and $g_{22}\sim\kappa^{-2}$. We see, that toroidal corrections die out very slowly and the true cylindrical limit is hardly achieved in real tokamaks.

For the opposite case of deeply trapped particles $\kappa<<1$, $g_{12}\sim\kappa$ and $g_{22}\sim\kappa^2$. Close to the trapped-passing boundary $\kappa=1$ all four elements of the diffusion tensor are of the same order of magnitude.

Consider now the $v_\perp$ dependence of the factor D_0 in Eq.(4.40). According to Eq.(4.14), $D_0 \sim v_\perp^{-3}$ at large $v_\perp$. One can also expect that D_0 vanishes rather rapidly at $v_\perp \to v_*$ since the LH spectrum is cut here very sharply. Then, introducing a normalized diffusion coefficient $\widetilde{D}_n = D_0 / v_*^2 \nu$ we can take, for the qualitative analysis, $\widetilde{D}_n(v_\perp)$ in the form

$$\widetilde{D}_n = D_n (v_* / v_\perp)^3 \qquad v_\perp > v_*$$

$$\widetilde{D}_n = 0 \qquad v_\perp < v_* \tag{4.41}$$

where D_n is a constant.

Substituting Eq.(4.41) into Eq.(4.26) and introducing non-dimensional variables

$$\omega = D_n^{-1/5} \frac{v_{\perp 0}}{v_*}, \quad u = D_n^{-1/5} \frac{v_{\|0}}{\sqrt{2\varepsilon} v_*} \tag{4.42}$$

we obtain:

$$\frac{\partial}{\partial u}\left(uF + \frac{g_{12}}{w^3}\frac{\partial F}{\partial w} + \frac{g_{22}}{w^3}\frac{\partial F}{\partial u}\right) + \frac{1}{w}\frac{\partial}{\partial w}\left(w^2 F + \frac{g_{12}}{w^2}\frac{\partial F}{\partial u} + \frac{g_{11}}{w^2}\frac{\partial F}{\partial w}\right) = Q \tag{4.43}$$

The tensor elements g_{ik} are now functions of the ratio u/w, therefore the left-hand side of Eq.(4.43) is independent of any numerical parameters. In the absence of the collisional velocity-space diffusion, the "active zone" $w>w_*$, where $w_* = D_n^{-1/5}$, can be considered independently of region $w<w_*$. The boundary conditions for the solution in the $w>w_*$ region are:

$$\Phi \to 0 \quad at \quad w \to \infty$$

$$g_{12}\frac{\partial \Phi}{\partial u} + g_{11}\frac{\partial \Phi}{\partial w} = 0, \quad at \quad w = w_* \tag{4.44}$$

$$\Phi = 0 \quad at \quad u = u_*$$

where

$$u_* = D_n^{-1/5}\frac{\sqrt{v_\alpha^2 - v_*^2}}{2\varepsilon v_*}$$

The second condition follows from the demand that Φ and $\mathbf{S}_\perp$ are continuous at $w=w_*$; the last one implies that the flux is dominated by collisional slowing-down at $u \geq u_*$. Suppose now that $u_* >> 1$ and consider the region $w>w_*$, $1<<u<u_*$, neglecting the diffusion tensor elements g_{12} and g_{22}, putting $g_{11}=1$, introducing $s = u/u_* = v_{ll}\sqrt{v_\alpha^2 - v_*^2}$ and the normalized distribution function

$$\Phi = \frac{N}{4\pi\mu v_\alpha^2}\Delta V_0 F$$

where $\Delta V_0 = \Psi' \Delta r T_B v_{ll0}/H_0$ is the shell volume at $\varepsilon \to 0$. Then Eq.(4.43) takes the form

$$\frac{\partial}{\partial s}\left(s\Phi\right) + \frac{1}{w}\frac{\partial}{\partial w}\left(w^2\Phi + \frac{1}{w^2}\frac{\partial \Phi}{\partial w}\right) = \delta\left(v - v_\alpha\right) \tag{4.45}$$

This equation is independent of ε and describes the cylindrical case. The general solution of Eq.(4.45) can be sought in the form

$$\Phi = \sum_n U\left(s\right)W_n\left(w\right) \tag{4.46}$$

where the functions W_n satisfy the equation

$$\frac{1}{w}\frac{d}{dw}\left[w^2 W_n + \frac{1}{w^2}\frac{dW_n}{dw}\right] + p_n W_n = 0 \tag{4.47}$$

Solutions vanishing at $w\to\infty$ are

$$W_n = C_n \frac{1}{w}\exp\left(-w^5/10\right) W_{\eta,q}\left(w^5/5\right) \tag{4.48}$$

where C_n is a constant, and $W_{\eta,q}$ are the Witteker functions with $\eta=(1+p_n)/5$ and $q=3/10$. The boundary condition $W_n'(w_*)=0$, following from Eq.(4.44), determines an infinite spectrum of positive eigenvalues p_n. The w_* dependence of several first eigenvalues found numerically is shown in Fig.3. At $w_*=0$ which means $D_n\to\infty$, we have $p_n=5n$. The eigenfunctions W_n are orthogonal and we suppose that they are normalized by

$$\int_{w_*}^{\infty} w e^{w^5/5} W_n W_m dw = \delta_{nm} \tag{4.49}$$

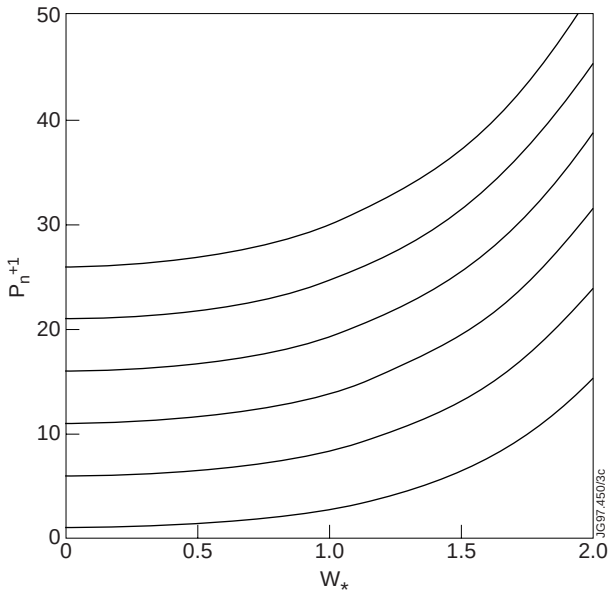

Fig.3. Eigenvalue spectrum of Eq. (4.47)

Consider now the functions $U_n(s)$ of Eq.(4.40). These functions satisfy the first-order equation

$$\frac{d}{ds}(sU_n) - p_n U_n = A_n(s) \tag{4.50}$$

where

$$A_n(s) = A\int_{w_*}^{\infty} we^{w^5/5} W_n \delta(v - v_\alpha) dw = \overline{A} e^{w(s)^5/5} W_n(w(s)),$$

$$\overline{A} = (v_\alpha / v_*^2 D_n^{2/5}) A \quad \text{and} \quad w(s) = \sqrt{v_\alpha^2 - (v_\alpha^2 - v_*^2)s^2} / D_n^{1/5} v_\alpha.$$

Solutions satisfying the boundary condition $U_n(1) = 0$ are

$$U_n(s) = s^{p_n - 1} \int_s^{\infty} x^{-p_n} A_n(x) dx \tag{4.51}$$

Consider this expression at large *n*. It can be shown, using the WKB approximation for the $W_n(w)$ functions with $n>>1$, that the factor $A_n(x)$ in Eq.(4.51) varies slowly compared to x^{-p_n}. Then Eq.(4.51) gives

$$U_n(s) \to \frac{A_n(s)}{p_n} \quad \text{n>>1} \tag{4.52}$$

Introduce

$$\Phi(s, w) = \sum_{n=0}^{\infty} \frac{A_n(s)}{p_n} \tag{4.53}$$

Then

$$\Phi = \Phi + \sum_{n=0}^{\infty} \left[U_n(s) - \frac{A_n(s)}{p_n} \right] W_n(w) \tag{4.54}$$

According to Eq.(4.52), the infinite sum in this expression converges rather rapidly, therefore, to a good approximation, only few first terms can be kept. A numerical analysis shows that a fairly good result is achieved even with the single n=0 term retained. Omitted terms then have a noticeable value only in the immediate vicinity of the boundary s=1; they just guarantee fulfillment of the boundary condition $\Phi(1)$=0. Since the function $A_0(s)$ is nearly constant over the integration region in Eq.(4.51), we have

$$\Phi = \Phi + \frac{\overline{A}}{1 - p_0} \left[s^{p_0 - 1} - \frac{1}{p_0} \right] \exp(w_*^5 / 5) W_0(w) W_0(w_*) \tag{4.55}$$

Recalling the definition of the function Φ, we conclude that it satisfies the ordinary differential equation

$$\frac{1}{w}\frac{d}{dw}\left[w^2\Phi_n + \frac{1}{w^2}\frac{d\Phi_n}{dw}\right] = \delta(v - v_\alpha) \tag{4.56}$$

with s entering as a parameter. Required solution of this equation is readily found by direct integration. The function Φ is a slowly varying function of the parameters and the s dependence of the distribution function $\Phi(s, w)$ is essentially determined by the second term in the left-hand side of Eq.(4.55). Its form depends on the eigenvalue p_0 which increases with the normalized diffusion coefficient $D_n = D_c / v_*^2 v$. This function is shown in Fig.4. At D_n>2.7, when p_0<1, the distribution has an integrable singularity at u=0. In this case, the small-v_{ll} fraction of the fast ion population is increased significantly. At D_n<2.7 the singularity vanishes and the distribution becomes more uniform.

This solution of the Fokker-Planck equation is valid in the cylindrical geometry. In the toroidal case it can be considered as an asymptotical solution in the passing particle domain. In accordance with its behaviour, one can expect a significant growth in number of trapped particles at D_n>2.7 and only a weak effect of the RF field on the α-particle population at smaller D_n.

Unfortunately, similar analysis for the trapped particles domain seems to be rather speculative. In the asymptotical region u>>w the Fokker-Planck equation has an infinite set of

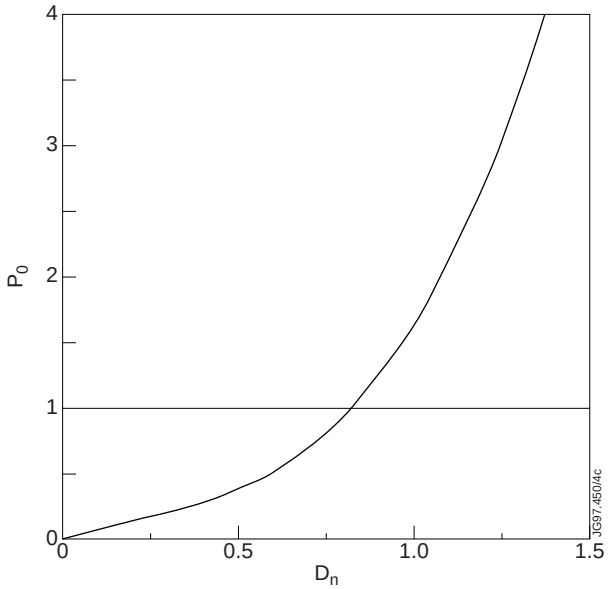

Fig.4. The fundamental eigemode p_0 *of Eq. (4.47) as a function of normalized diffusion coefficient* D_n.

particular solutions of the form $\Phi_n = u^{p_n} W_n(w)$ where W_n are again expressed in terms of the Witteker functions. However, the spectrum now includes eigenvalues p_n of both signs, the eigenfunctions W_n are not orthogonal and completeness of the system is an open question. Assuming, nevertheless, that the solution is dominated by an eigenfunction with the smallest positive eigenvalue (which appears to be close to unity) we obtain a reasonable, nearly uniform,

distribution of deeply trapped particles over v_{ll}. An absolute value of the distribution function here can be found demanding that the calculated flux across the boundary $v_{\perp} = v_{*}$ to be in agreement with the source of the particles. Asymptotical solutions found in this way at small and large u, can be connected by a smooth monotonic curve across the trapped-passing boundary.

5. NUMERICAL RESULTS AND CONCLUSIONS

In this section we illustrate the actual behaviour of the distribution function F by a numerical example for an imaginary JET shot with central electron temperature T_{eo}=4.3keV, central ion temperature T_{io}=20keV, central plasma density n_{eo}=1.9×10^{19}m^{-3} and RF power P_{LH}=6Mw. In Figs 5a-5c the elements of normalized diiffusion tensor D_{ik} are shown as functions of $v_{\perp 0}$ and v_{ll0}.

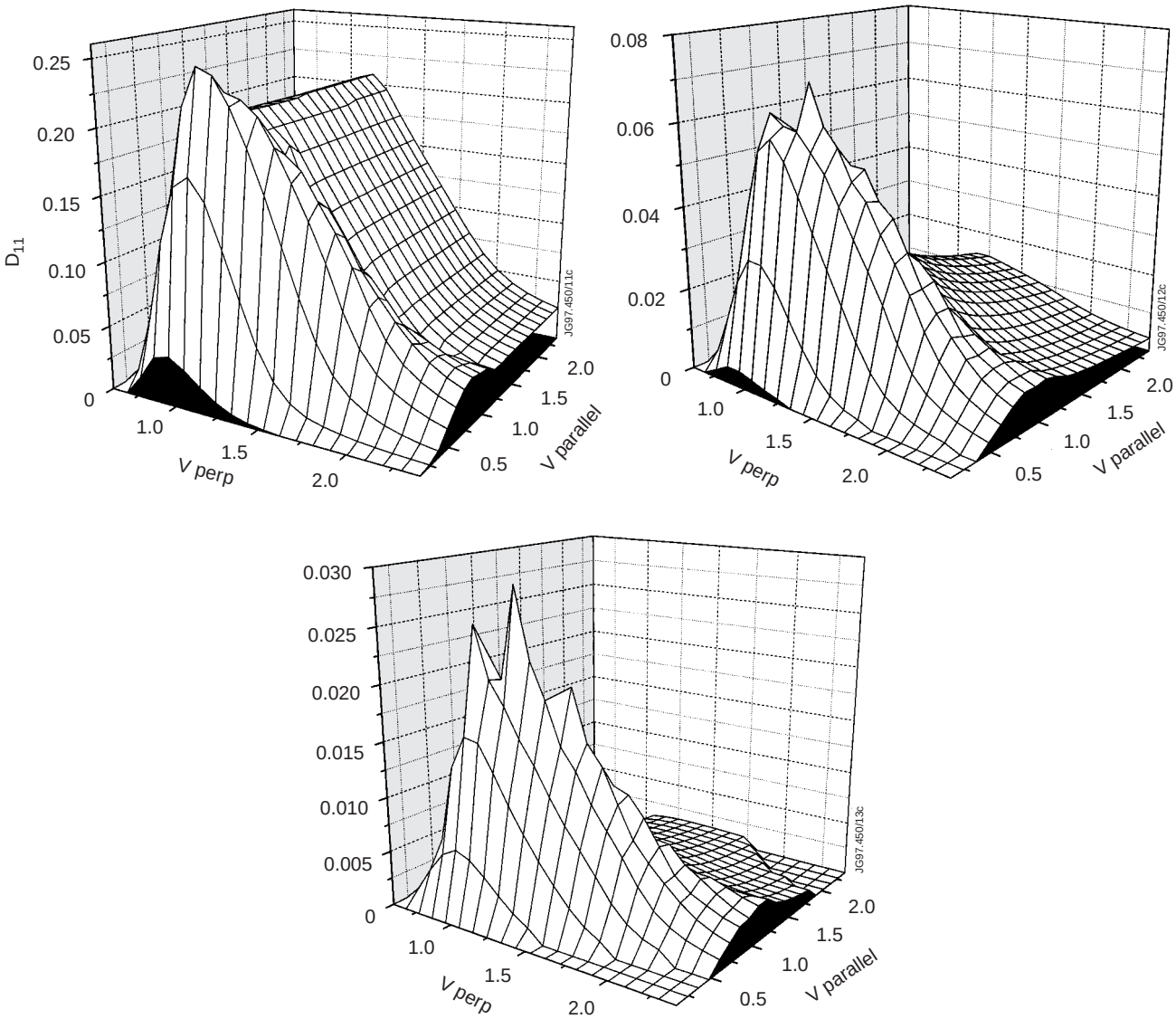

Fig.5. Elements of the normalized diffusion tensor D_{ik}*; velocities are measured in units of alpha particle birth velocity. a)* D_{11}*, b)* D_{12}*, c)* D_{22}*.*

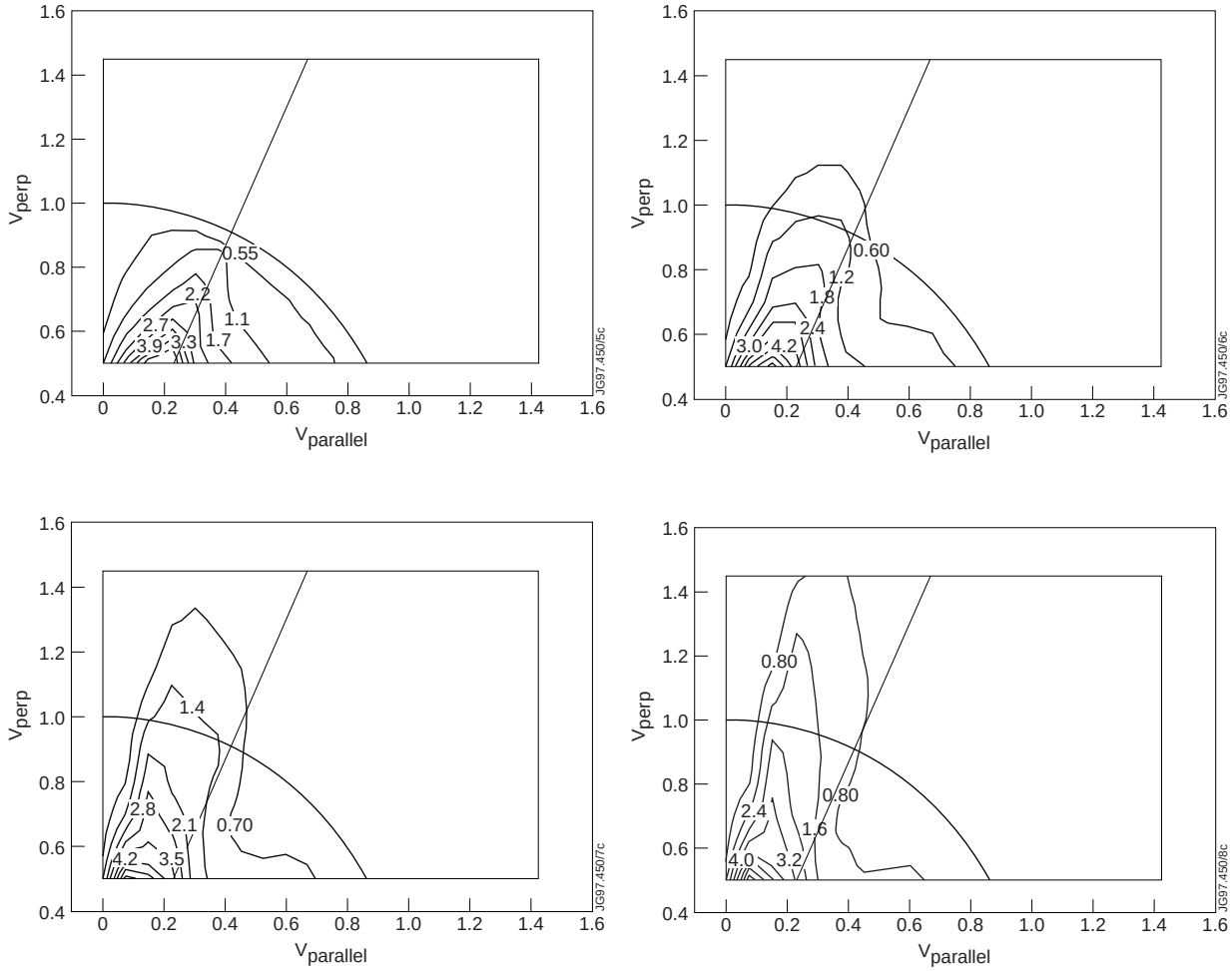

Fig.6. Contours of the distribution function F *in the* ($v_\perp$,v_{ll}) *plane for various values of the magnification factor* χ*: a)* χ*=0, b)* χ*=1, c)* χ*=2, d)* χ*=4. The direct line indicates the trapped-passing boundary, the figures denote relative values of the* F *function.*

Their shapes are in qualitative agreement with the above analysis, however, “toroidal” elements D_{12} and D_{12} appear to be several times smaller then the “cylindrical” element D_{11}. To illustrate the RF power effect on the distribution function, we have solved Eq.(4.31) with the above diffusion tensor multiplied by a constant factor χ for various values of this parameter. Results for χ=0, 1, 2 and 4 are presented in Figs.6a-6d. One can see that the distribution function has no spherical symmetry in co-ordinates $v_{\perp 0}$, v_{ll0} even in the absence of the RF power. Formation of the fast particle tail with the groth of the quasilinear diffusion is predominantly observed in the trapped particle region. This effect is again illustrated in Fig.7. Finaly, Fig.8 shows the function $f_\alpha(v_\perp, \theta)$ which determines the α-particle wave damping.

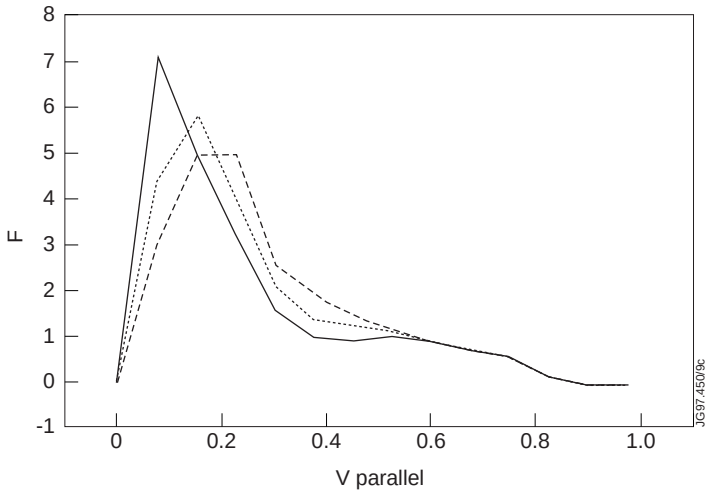

Fig.7. The distribution function F vs. v_{ll} *at* $v_{\perp}=v_{*}$. *Broken line* $\chi=0$, *dashed line* $\chi=1$, *solid line* $\chi=4$.

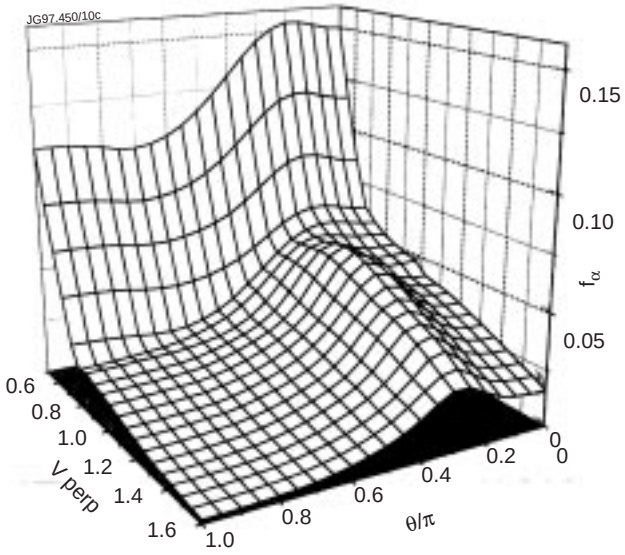

Fig.8. One-dimensional distribution function f_α ($v_\perp$,θ) *for* $\chi=4$.

Principal conclusions one can draw from results of this work are that:

1. The quasilinear diffusion of fast ions interacting with the LH waves is essentually two-dimensional.
2. A cylindrical model is a poor approximation for the fast ion minority in real tokamaks.
3. The most important effect of LH waves on the α-particle population is, probably, an increase of the trapped particle fraction which can influence the plasma stability. However, no large change in the α-particle wave damping due to the toroidal effects can be expected. This means, taking into account a fairly small α-particle contribution to the total wave damping, that a simple 1D model can be, after all, used in self-consistent ray tracing calculations. This assumption will be tested in a future work.

ACKNOWLEDGEMENTS

This work has been carried out under JET Contract No. JJ6/11906. We would like to thank Dr. F.X.Sîldner who has initiated and encouraged this work. Also we wish to thank Dr. Yu.F.Baranov for helpful attention during our work at JET.

REFERENCES

1. A.Esterkin, A.Piliya "Fast ray tracing code for LHCD simulations", *Nuclear Fusion,* Vol.36, No.11, p.1501-1512, (1996).
2. N.J.Fish, J.M.Rax "Current drive by LH waves in the presence of energetic alpha particles", *Nuclear Fusion,* Vol.32, No.4, p.549, (1992).

3. W.H.Press, et al. “Numerical Recipes”, Cambridge University Press, Cambridge, (1986), 627 pp.

4. E.Barbato, F.Santini “Quasi-linear absorption of lower hybrid waves by fusion generated alpha particles” *Nuclear Fusion,* Vol.31, No.4, p.673, (1991).